

VISCOELASTIC FLOW OF BOGER FLUIDS IN A 4:1 SQUARE/SQUARE CONTRACTION

Manuel António Alves

Departamento de Eng^a Química, CEFT, Faculdade de Engenharia da Universidade do Porto, Rua Dr. Roberto Frias s/n, 4200-465 Porto, Portugal
mmalves@fe.up.pt

Fernando Tavares de Pinho

Centro de Estudos de Fenómenos de Transporte, Dep. Eng. Mecânica, Universidade do Minho, Campus de Azurém, 4800-058 Guimarães, Portugal
fpinho@dem.uminho.pt

Paulo Jorge Oliveira

Dep. Eng. Electromecânica, Unidade de Materiais Têxteis e Papeleiros, Universidade da Beira Interior, 6201-001 Covilhã, Portugal
pjpo@ubi.pt

Abstract. Visualizations of the 3-D flow in a 4:1 square-square sudden contraction were carried out for two Boger fluids with different degrees of elasticity (100 and 300 ppm of polyacrylamide (PAA) in 91% glycerine, 7.5% water and 1.5% NaCl), under conditions of negligible inertia ($Re_1 < 0.1$). The rheology of the fluids was well characterised in steady and oscillating shear flows prior to the fluid dynamic investigations, based on streak-line photography and laser light illumination. For both PAA solutions the length of the recirculation region in the middle plane has a non-monotonic variation with flow elasticity. Initially, x_R/H_1 increases at low Deborah numbers to a maximum at about $De_1=0.1$, then it decreases as De_1 tends to 0.2. For the less elastic fluid (PAA 100) the vortex even disappeared whereas for the PAA 300 fluid a minimum $x_R/H_1 \approx 0.15$ was observed. As flow elasticity increased further, a tendency was observed for divergence of the streamlines approaching the contraction plane prior to a significant increase in vortex length. Values of x_R/H_1 exceeded 0.9, as Deborah number reached about $De_1 \approx 0.7$ to 0.8, when elastic instabilities set in leading to periodic unsteady flow.

Keywords. Boger fluids, 3D sudden contraction, viscoelasticity, vortex growth, unsteadiness

1. Introduction

Sudden contraction flows are classical benchmark problems in computational rheology (Hassager, 1988), and a large number of visualization studies in planar and axisymmetric contractions have been published in the literature. In these simple configurations, the flow behaviour of non-Newtonian fluids can be very surprising, and different flow patterns have been observed even for fluids with apparently similar rheological properties.

The first visualizations in circular contractions for viscoelastic fluids were carried out by Cable and Boger (1978a, 1978b, 1979) and Nguyen and Boger (1979), who reported a dramatic growth of the salient corner vortex for shear rates higher than a critical value above which the normal stress grew quadratically. These experiments were performed for contraction ratios in the range 7.67:1 to 14.83:1 and at very high Weissenberg numbers the flow became asymmetric and eventually time-dependent. In 1986 Boger et al investigated the behaviour of Boger fluids with similar steady and dynamic shear properties and found different vortex dynamics, thus concluding that a different fluid property had to be taken into account. In his 1987 review paper Boger suggested extensional viscosity as that property, and described in some detail the sequence of flow dynamics in the sudden contraction. For some fluids, only a corner vortex exists, which grows in size as elasticity increases whereas for other fluids the corner vortex extends to the re-entrant corner near which a lip vortex is formed. For high contraction ratios the two vortices are initially separate, as also seen by McKinley et al (1991) in his 4:1 contraction experiments. As the elasticity increased the lip vortex grew at the expense of the corner vortex, while the length of the recirculation remained fairly constant. Eventually, the lip vortex occupied the whole contraction plane region and a further increase in the Weissenberg number lead to an increase of the now concave shaped vortex. At higher Weissenberg numbers a small pulsating lip vortex appeared and lead to unsteady behaviour.

The relevance of extensional viscosity was also emphasized in the experimental investigations of White and Baird (1986) in a planar contraction with polystyrene (PS) and low density polyethylene (LDPE): whereas a vortex was found for the LDPE, it was absent from PS and the difference was attributed to their different extensional viscosities. This was further emphasised when they used later (White and Baird, 1988) a constitutive equation that represented correctly the measured extensional viscosity of both fluids and were able to numerically predict the different vortex patterns observed in 1986. In the mid 1980's the experimental work on the 4:1 contraction flow concentrated on assessing the various flow transitions and instabilities and used several experimental techniques, as in McKinley et al (1991).

Soon after the beginning of the experimental investigations on axisymmetric contraction flows, the effect of different contraction geometries was also assessed. Flow in planar contractions were experimentally studied as early as 1982 by Walters and Webster, who found no significant vortex activity for Boger fluids in the 4:1 case, in marked contrast to observations in 4.4:1 circular contractions. However, for shear-thinning fluids the vortex activity was significant in both planar and axisymmetric geometries. To help clarify these differences, Evans and Walters (1986) forced shear-thinning elastic fluids through various planar contractions (contraction ratios of 4:1, 16:1 and 80:1) to find vortex enhancement even in the smaller contraction and its intensification with both contraction ratio and fluid elasticity. For the larger contraction, however, a lip vortex was found and a growth mechanism similar to that found for circular dies was seen, whereas in the 4:1 contraction only the corner vortex was observed. In 1988 Evans and Walters looked at the behaviour of Boger fluids in the 4:1 contraction to find a small lip vortex, but without a connected corner vortex. Both the corner and lip vortices were reduced and here fluid inertia played a critical role. This independence of lip and corner vortices has also been found recently, in the numerical simulations of Alves et al (2003a) for Boger fluids represented by the Oldroyd-B model. Detailed experiments, including velocity measurements by LDA, were carried out by Quinzani et al (1994) for the 4:1 planar geometry.

The surprisingly different behaviours of Boger fluids in circular and planar contractions has been recently confirmed by the careful experiments of Nigen and Walters (2002): experiments were conducted with both Newtonian and Boger fluids having identical shear viscosities and it was quite clearly demonstrated that, although there were higher extensional strain rates in the planar geometry than in the circular die, virtually no vortex enhancement was found in the former geometry whereas dramatic vortex enhancement for the Boger fluids was found in the latter.

Flow in square-square contractions has captured less attention, but by no means is unknown: Walters and Webster (1982) basically found similarities between the flows through circular and square-square contractions, whereas the differences between the flows in planar and circular contractions were confirmed by Walters and Rawlinson (1982) to occur also between planar and 13.3:1 square-square contractions. The experiments and numerical calculations of Purnode and Crochet (1996) also found similarities between the main flow features in 2D and 3D flows, and they concluded that lip vortices should not be associated with inertial effects. However, these authors also found that full capture of three-dimensional effects required 3D computations and especially an accurate representation of fluid rheology. In this geometry, and in contrast to the 2D planar case, the pressure can close in the tangential direction as for the axisymmetric geometry, but the loss of axisymmetry leads to normal stress imbalances that create secondary flows and the dynamics of the vortices in combination with the secondary flow structures and fluid elasticity are still to be understood.

In conclusion, it is clear that much less is known for the square-square contraction than for the circular or 2D planar contractions, and this is the motivation of the present work, which concentrates on general characteristics of the flow for elastic fluids of constant viscosity. In the next Section the experimental apparatus, the experimental techniques and the rheology of the fluids are discussed in detail. Then, in Section 3, results of the visualizations are presented and discussed prior to closure of the paper.

2. Experimental conditions

2.1. Experimental rig

The experimental apparatus is schematically depicted in Fig. 1(a). The rig consisted of two consecutive square ducts of length 1000 mm and 300 mm, having sides of $H=24.0$ mm and $h=6.0$ mm, respectively, thus defining the 4:1 contraction ratio, and a vessel. The flow rate was set by an adequate control of applied pressure on the upstream duct and frictional losses in the long coiled pipe located between the duct and the vessel, at the bottom of the rig. To achieve low flow rates this coiled 8 m long pipe had a diameter of 4 mm, whereas for higher flow rates a larger 6 mm diameter coiled pipe was used. Applied pressure was kept between 0.5 and 4 bar and the dashed lines in Fig. 1(a) represent the pressurised air lines. The flow rate was measured by a stop-watch and the passage of the liquid free-surface at two marks in the upper duct. In all tests the fluid temperature was measured and the fluid properties were taken from the rheometric master curves shown in the next section.

A 10 mW He-Ne laser light source was used to visualise the flow patterns. The laser beam passed through a cylindrical lens to generate a sheet of light illuminating highly reflective tracer particles suspended in the fluid (10 μ m PVC particles, circa 15 mg/kg fluid). The streaklines were recorded using long time exposure photography with a conventional camera (Canon EOS300 with a macro EF100 mm f/2.8 lens), as sketched in Fig. 1(b), which includes a schematic representation of the test section.

2.2. Rheological characterisation of the fluids

Four fluids based on mixtures of glycerine and water were investigated: two viscous Newtonian fluids (designated by N85 and N91) and two Boger fluids (PAA100 and PAA300). Their compositions and the corresponding densities are listed in Tab. (1). The Boger fluids were prepared by dissolving a small amount of polyacrylamide (PAA - Separan AP30 produced by SNF Floerger) in the Newtonian solvent N91. To minimize the intensity of shear-thinning, a small

amount of NaCl is used, as described in detail in Stokes (1998). To avoid bacteriological degradation of the solutions, a biocide was also added (Kathon LXE from Rohm and Haas). The fluid densities were measured at 21.2°C with a picnometer.

The shear viscosity (η) and the first normal stress difference coefficient (Ψ_1) in steady shear flow, and the rigidity and loss moduli (G' , G'') in dynamic shear flow were used to characterize the rheology of the Boger fluids. These properties were measured by an AR2000 rheometer from TA Instruments, using a cone-plate set-up with 40 mm diameter and 2° angle. A falling ball viscometer from Gilmont Instruments (ref. GV-2200) was also used for some viscosity measurements with the Newtonian fluid.

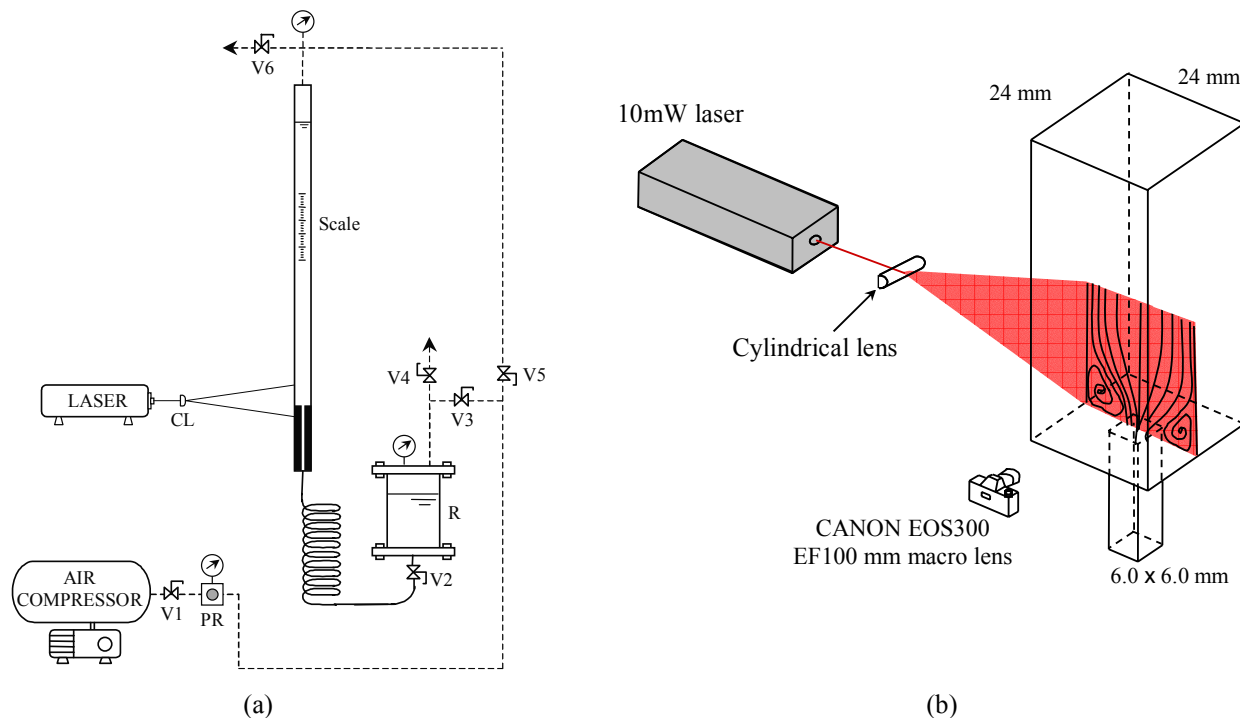


Figure 1- Experimental flow rig: (a) Schematic representation of rig (PR- pressure regulator; V1 to V6- ball valves; R- reservoir; CL- cylindrical lens); (b) Flow visualization technique and test section.

Table 1- Composition and properties of fluids (mass concentrations).

Designation	PAA [ppm]	Glycerine [%]	Water [%]	NaCl [%]	Kathon [ppm]	ρ [kg/m ³]	η_0 [Pa.s]
N85	-	84.99	15.01	-	25	1221	0.125
N91	-	90.99	7.51	1.50	25	1250	0.366
PAA100	100	90.99	7.50	1.50	25	1249	0.520
PAA300	300	90.97	7.50	1.50	25	1247	0.740

2.2.1. Newtonian fluids

For the N85 and N91 fluids the shear viscosities were $\eta = 0.125$ Pa.s and 0.366 Pa.s at 18°C and 20°C, respectively, the temperatures at which the visualizations took place. Fluid N91, which served as solvent for the PAA solutions, was also used to evaluate the accuracy of the instrument and to establish the base noise level in dynamic tests. For shear rates between 1 and 1000 s⁻¹, the viscosity of fluid N91 was correctly measured and varied less than 2%, well within experimental uncertainty. For N_1 , the measurements at $\dot{\gamma} < 100$ s⁻¹ indicated zero reading within experimental uncertainty, as it should. The uncertainty in measuring N_1 is of the order of ± 10 Pa, in agreement with the specifications of the manufacturer for the cone-plate geometry used. For $\dot{\gamma} > 100$ s⁻¹ inertial effects become important and N_1 becomes negative. The effect of inertia on N_1 for Newtonian fluids is well quantified by $N_{1,inertia} = -0.15\rho\omega^2R^2$ (Barnes, 2000), but these results are not shown here for conciseness (more details in Alves, 2004).

The effect of temperature on the shear viscosity for the N91 fluid is well predicted by an Arrhenius equation, defining a shift factor a_T of the form

$$\ln(a_T) = \ln\left(\frac{\eta}{\eta_0}\right) = \left[\frac{\Delta H}{R}\left(\frac{1}{T} - \frac{1}{T_0}\right)\right] \quad (1)$$

where η_0 represents the viscosity at the reference absolute temperature T_0 , and the fitting of this equation to the experimental data gave $\Delta H/R = 6860$ K (more details in Alves, 2004).

2.2.2. Boger fluids

For the Boger fluids the steady shear properties were measured at temperatures ranging from 15.3° C to 30° C, and the time-temperature superposition technique was found to be valid for both Boger fluids and used to build master curves with the same estimated value of $\Delta H/R$ as for the solvent. The reduced shear data are plotted as symbols in Figs. 2(a) and 2(b) for the PAA100 and PAA300 fluids, respectively. Both figures include dynamic shear data in appropriate form ($\eta'_r, 2G'_r/\omega_r^2$ vs. ω_r) in order to compare the corresponding limiting behaviour at vanishing deformations. The lines represent predictions by three-mode Oldroyd-B constitutive equations that were fitted to the experimental data. The parameters of these fitted Oldroyd-B models are listed in Tab. (2), at reference temperature.

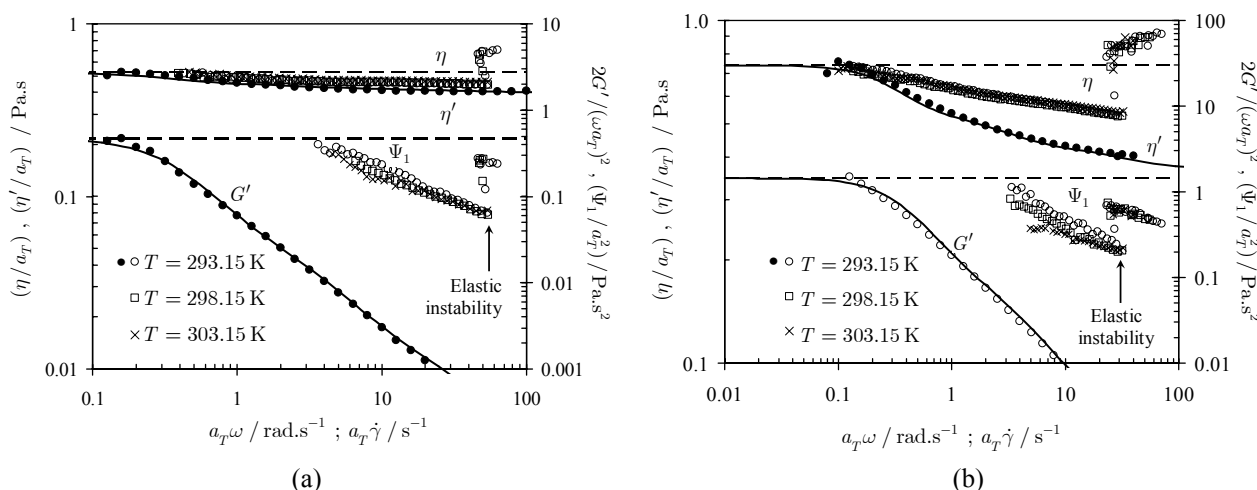


Figure 2- Material parameters in steady (η, Ψ_1) and oscillating (G', η') shear flow for the Boger fluids: (a) PAA 100; (b) PAA 300. Lines represent fitting by a three-mode Oldroyd-B model.

Table 2- Linear viscoelastic spectra for the Boger fluids at $T_0 = 293.15$ K.

Mode k	λ_k [s]	η_k [Pa.s]	
		PAA100	PAA300
1	3.0	0.075	0.23
2	0.3	0.027	0.09
3	0.03	0.018	0.05
solvent	-	0.40	0.37

The data in Figs. 2(a) and 2(b) show well the limiting behaviour of the properties measured in steady and oscillating shear flows. The reduced shear viscosity is approximately constant at reduced shear rates in the range 0.3 to 50 s^{-1} for the PAA100, whereas for the PAA 300 it decreases approximately 10% per decade of reduced shear rate. At $\dot{\gamma}_r = 54 s^{-1}$ and 28 s^{-1} (for the PAA 100 and PAA 300, respectively) there is an abrupt growth in η_r and Ψ_{1r} , and this is accompanied by a slight reduction in reduced shear rate (with the rheometer operating in “controlled stress mode”). This phenomenon results from an elastic instability leading to three-dimensional flow, which is typically observed with Boger fluids in cone-plate and plate-plate flows, as investigated previously by Phan-Thien (1985) and McKinley et al (1991). The three-mode Oldroyd-B model is accurate enough to predict G' and G'' within the measured range. Data at low and high frequencies, leading to values of G' close to the base line, were excluded. The spectrum will be useful later to help quantify the Deborah number and for future numerical simulations of this flow.

3. Flow visualization results

3.1. Newtonian fluids

Flow visualizations were carried out first with Newtonian fluids to assess the effect of inertia and for comparison purposes with the results of the elastic Boger fluids. Fig. 3 shows stream-traces of the flow of the Newtonian fluid N91 in the middle plane of the 3D sudden contraction and Fig. 4 plots the variation of the normalised vortex length with

Reynolds number, measured with both Newtonian fluids in the same plane. The Reynolds number is defined as $Re_1 = \rho H_1 U_1 / \eta$.

As expected, inertia leads to a reduction of the corner vortex, especially for Reynolds numbers above 0.05. At low Reynolds numbers, inertial effects are negligible and x_R/H_1 asymptotes to 0.326, where H_1 represents the upstream duct half-width. Under creeping flow conditions, note that for a 4:1 circular contraction $x_R/H_1 \rightarrow 0.326$ also, while for a 4:1 planar contraction $x_R/H_1 \rightarrow 0.375$ (see Alves et al, 2003b). Even though, at first sight, the flow inside the vortex looks two-dimensional, in reality it is three-dimensional and, in contrast with the planar and axisymmetric sudden contraction flows, none of the recirculations are ever closed in the square contraction as seen by a closer inspection of the streaklines.

For Newtonian fluids, all the experimental flow features are well captured by numerical simulations shown in the predicted variation of the vortex length with the Reynolds number in Fig. 4. These numerical simulations are shown in Alves (2004), and were obtained with a finite-volume code developed by the authors (Alves et al, 2003a).

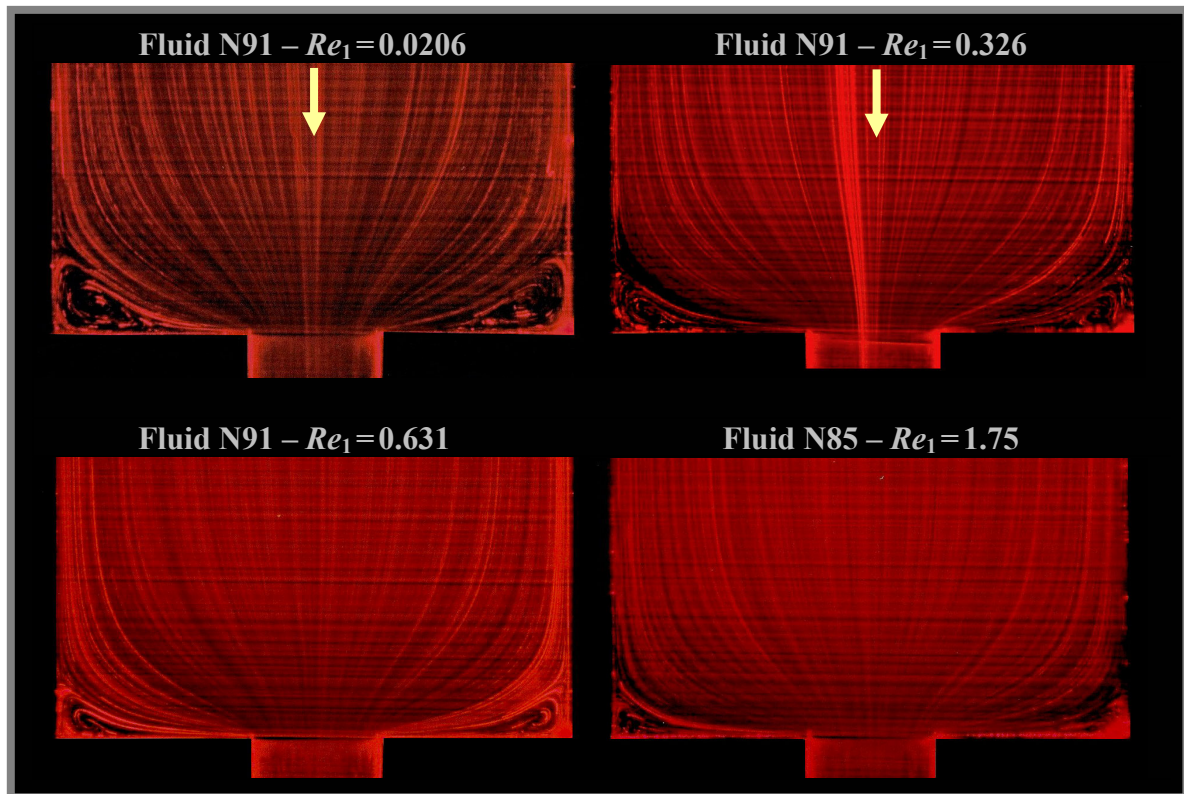


Figure 3- Streaklines for the flow of Newtonian fluids in the middle plane of a 4:1:1 sudden contraction.

3.2. Boger fluids

To quantify the strength of elastic effects with Boger fluids it is convenient to use a single relaxation time in the definition of the Deborah number,

$$De_1 = \frac{\lambda_p(T) U_1}{H_1} = \frac{a_T \lambda_p(T_0) U_1}{H_1} \quad (2)$$

In this equation λ_p is Oldroyd's relaxation time, which is calculated from the linear viscoelastic spectrum using Eqs. (3 a,b). In this way, it is guaranteed that at low rates of deformation (low angular velocities), the viscoelastic behaviour of the equivalent single mode model is identical to that of the multimode UCM plus Newtonian solvent model (e. g. $\Psi_{1,0} \equiv \lim_{\dot{\gamma} \rightarrow 0} \Psi_1 = \sum_k 2\eta_k \lambda_k = 2\eta_p \lambda_p$).

$$\eta_p = \sum_{k \neq \text{solvent}} \eta_k \quad \text{and} \quad \lambda_p = \sum_{k \neq \text{solvent}} \frac{\eta_k \lambda_k}{\eta_p} \quad (3 \text{ a,b})$$

Hence, from data in Tab. (2), the parameters of the equivalent single mode Oldroyd-B model are the following: PAA100 — $\eta_0 \equiv \eta_s + \eta_p = 0.52$ Pa.s, $\beta \equiv \eta_s/\eta_0 = 0.769$ and $\lambda_p = 1.947$ s; PAA300 — $\eta_0 \equiv \eta_s + \eta_p = 0.74$ Pa.s, $\beta \equiv \eta_s/\eta_0 = 0.5$ and $\lambda_p = 1.942$ s.

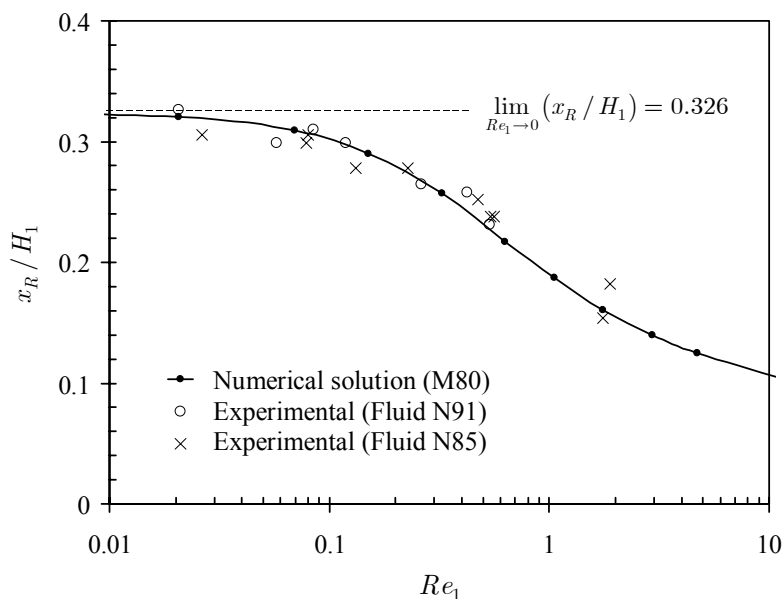


Figure 4- Influence of the Reynolds number on the vortex length at the middle plane of a square-square 4:1:1 sudden contraction for Newtonian fluids N85 and N91. Comparison between experiments and numerical predictions.

Streaklines at the middle plane of the contraction are presented in Fig. 5 for the flow of the PAA100 fluid for increasing values of the flow rate. The flow characteristics are complex, but with $Re_1 < 0.11$ inertial effects are negligible and thus the complex behavior observed is mainly caused by elastic effects. At low values of the Deborah number ($De_1 = 0.041$), viscous effects predominate and the flow pattern is similar to that seen in Fig. 3 for Newtonian fluids, with the separation pathline still concave in shape. With increasing Deborah number changes progressively occur: first, there is a very slight increase in vortex size while the separation pathline straightens, then the corner vortex progressively decreases in size to about a quarter at $De_1 \approx 0.2$, an effect not due to inertia since the Reynolds number remains lower than 0.05. Note that for the 4:1 axisymmetric contraction, McKinley et al (1991) reported results bearing some resemblance: negligible elastic effects for $De_2 < 1$ and a decrease in the corner vortex up to $De_2 = 3.4$, based on downstream flow quantities (their, as in here $De_2 = 64De_1$). However, in contrast to McKinley et al, the formation of a strong lip vortex while the corner vortex decreases is not seen here, although the higher curvature of the streaklines at the reentrant corner suggests the possibility of a weak lip vortex there (see photo for $De_1 = 0.210$).

As the Deborah number further increases the corner vortex starts to grow, and simultaneously the mid-plane streamlines approaching the contraction plane progressively diverge with flow elasticity ($De_1 \geq 0.376$). This anomalous effect had already been predicted by Alves et al (2000) for the flow of a Boger fluid in a 4:1 plane sudden contraction (see their Figure 7 at $De = 5$) and was also observed by McKinley et al (1991) for the flow of Boger fluids in circular contractions. This streamline divergence upstream of the contraction for Boger fluids can be attributed to a local intense increase in extensional viscosity leading to an increased flow resistance just upstream of the contraction plane as the extension rates grow in a region of predominantly extensional flow characteristics. This extensional thickening is characteristic of Boger fluids, but there are not enough data to correlate rheological behavior with diverging flow. McKinley et al (1991) discusses this issue and mentions different diverging flow intensities for fluids with similar extensional viscosity behavior, and argues for the relevance of the total Hencky strain to this flow feature. Of note here, the diverging streamlines with Boger fluids were observed in the absence of noticeable lip vortex activity. This contrasts with the visualizations of McKinley et al (1991) in the axisymmetric geometry, but agrees with their conclusions that diverging streamlines and lip vortex are unrelated.

The growth of the large vortex continues with elasticity, and the flow remains steady up to Deborah numbers of the order of 0.8. As the Deborah number further increases the flow becomes periodic, possibly due to an elastic instability and this is observed in the crossings of some streaklines for $De_1 = 0.847$. The amplitude of the oscillations increase with De_1 and this can be seen in the three snapshots of Fig. 6, taken at different moments within a cycle for one supercritical flow condition. At higher flow rates the flow eventually loses its periodicity.

For the second Boger fluid, PAA300, the pathline flow visualizations are shown in Fig. 7. In general terms, the influence of elasticity is the same as for PAA100, but there are important differences worth mentioning. First, the increase of the middle-plane corner vortex at low Deborah numbers is also observed, but is now significantly more

intense than with PAA100, as can be properly assessed in the plot of x_R/H_1 versus De_1 in Fig. 8: x_R/H_1 peaks by more than 25% relative to the Newtonian value at $De_1 \approx 0.08$. Then, x_R/H_1 decreases to about 0.15 in the range $De_1 = 0.1$ to 0.2, but the other main difference relative to PAA100 is that now the middle-plane vortex has changed from a corner vortex to a lip vortex (see photo at $De_1 = 0.149$), which has similarities to that found numerically for Boger fluids in the 4.1 plane contraction by Alves et al (2000) (cf. their Figure 7 at $De = 4$ for UCM fluids).

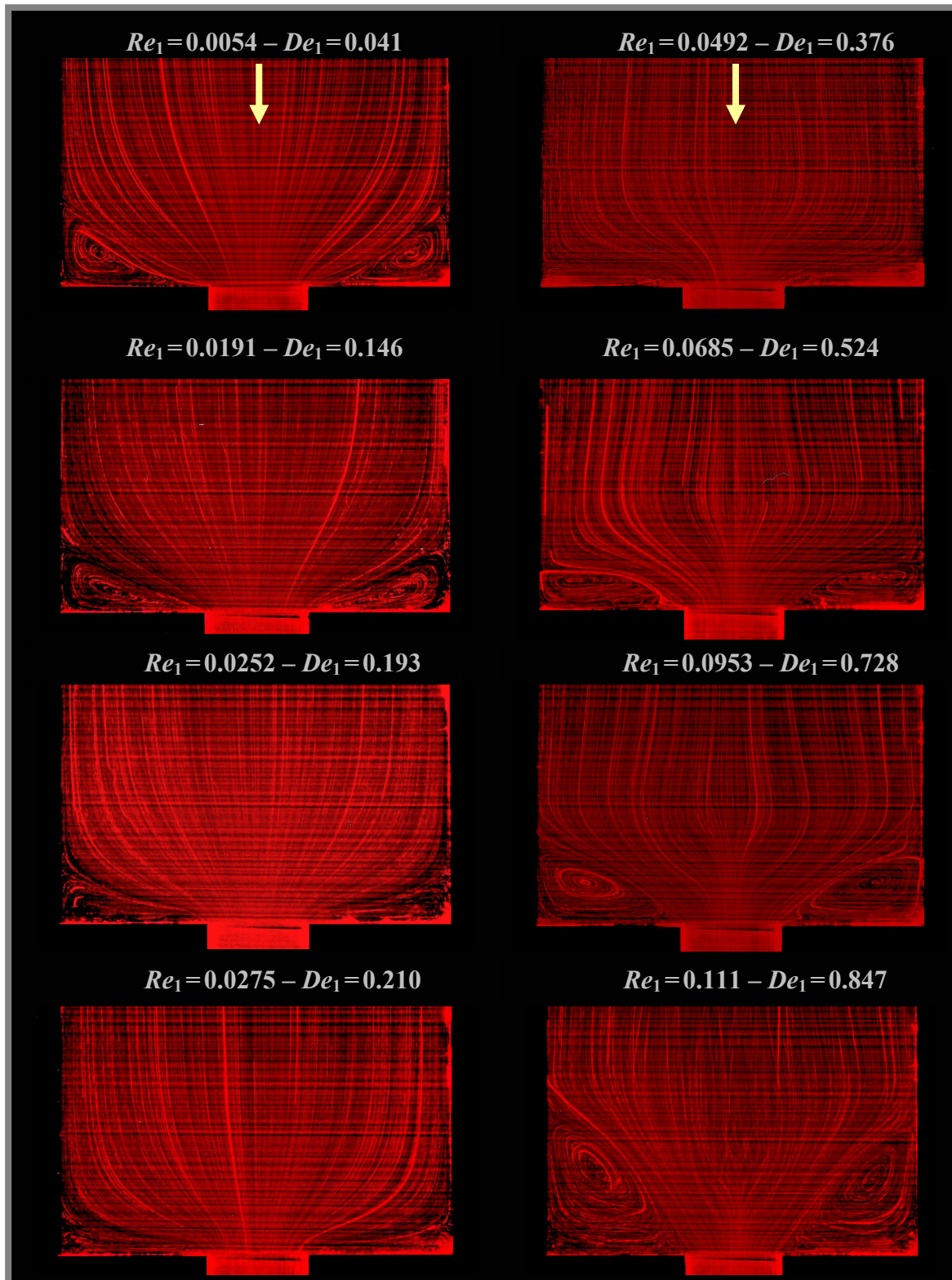


Figure 5- Influence of elasticity on the streakline flow patterns at the middle plane of a 4:1:1 sudden contraction for PAA 100.

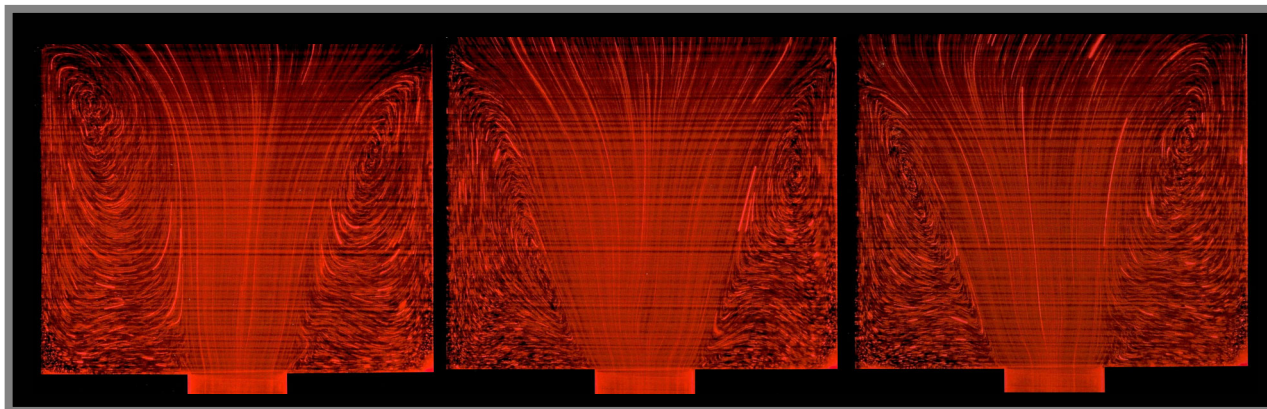


Figure 6- Streaklines for the flow of PAA 100 in the middle plane of a square-square contraction at three different moments within one different oscillating supercritical flow condition ($De_1 = 1.22$).

It is known from experimental and numerical work in the 4:1 plane sudden contraction flow with Boger fluids (Nigen and Walters, 2002; Walters and Webster, 2003), that a lip vortex is formed at low to moderate Deborah numbers. This lip vortex grows with elasticity and eventually dominates the corner vortex that is so characteristic of low Deborah number flows. In contrast, for the axisymmetric sudden contraction flow of Boger fluids, often the corner vortex grows with elasticity without any lip vortex, but there are exceptions such as those reported by Boger et al (1986) and especially McKinley et al (1991) with PIB/PB solutions (polyisobutylene in polybutene). Although the square/square contraction has similarities to the axisymmetric geometry, because of the extensional strain rates and the possibility of partial balance of cross-stream pressure and stress gradients, the visualizations of Evans and Walters (1986) for a square/square 16:1:1 contraction do not show any lip vortex, but only enhancement of the middle-plane corner vortex, in deep contrast to our results for the PAA300 fluid (but in agreement with our results for PAA100).

Vortex enhancement with elasticity occurs for $De_1 > 0.3$, but now this refers to the lip vortex rather than the corner vortex found for the PAA 100, and is much stronger. As with the PAA100, there are diverging streaklines upstream of the contraction plane, but now in the presence of a lip vortex. The appearance of diverging streaklines in a 3D square/square contraction flow of Boger fluids, with and without lip vortex, is here documented for the first time and confirms the suggestion of McKinley et al (1991) that the two phenomena are unrelated.

At even higher Deborah numbers, such as at $De_1 = 0.726$, the flow of PAA300 also becomes periodic as the flow of PAA100. This periodicity results from an elastic instability and occurs earlier than for the PAA100 solution, at $De_1 \approx 0.7$.

4. Conclusions

Flow visualisations were carried out in the middle plane of a 4:1:1 sudden square/square contraction for Newtonian and Boger fluids under conditions of negligible inertia, using streakline photography. The Newtonian flow patterns were in good agreement with numerical results and showed inertia to be negligible for Reynolds numbers below 0.05. The flowfield was clearly three-dimensional with open recirculations, and inertia pushed the corner vortex towards the contraction plane, as expected.

For the two Boger fluids the recirculations were seen to increase at low Deborah numbers, prior to an intense decrease leading to a minimum size at $De_1 \approx 0.2$. Then, as elasticity increased further, the streaklines on the central region of the approaching flow started to diverge while the vortices grew again with elasticity in a much stronger way, until the flow became periodic and eventually chaotic at very high flow rates. For the more concentrated Boger fluid (PAA300) these effects were stronger in magnitude due to its higher elasticity, but a major difference in flow features was seen: after the vortex got small at low Deborah numbers, a lip vortex appeared and grew with elasticity in contrast to the PAA100 solution, where only corner vortex enhancement was observed. This conflicting behaviour, and the existence of diverging flow upstream of the contraction, are here reported for the first time in the square/square contraction flow of Boger fluids. However, similar flow features have been reported in the past for the circular contraction, as is discussed.

5. Acknowledgements

The authors would like to thank Prof. M. P. Gonçalves and Mr. D. Torres for their help in characterizing the rheology of the fluids used in this work. M.A. Alves wishes to thank Fundação Calouste Gulbenkian for financial support. Sponsorship of FEDER via FCT program POCTI/37711/EME/2001 is gratefully acknowledged.

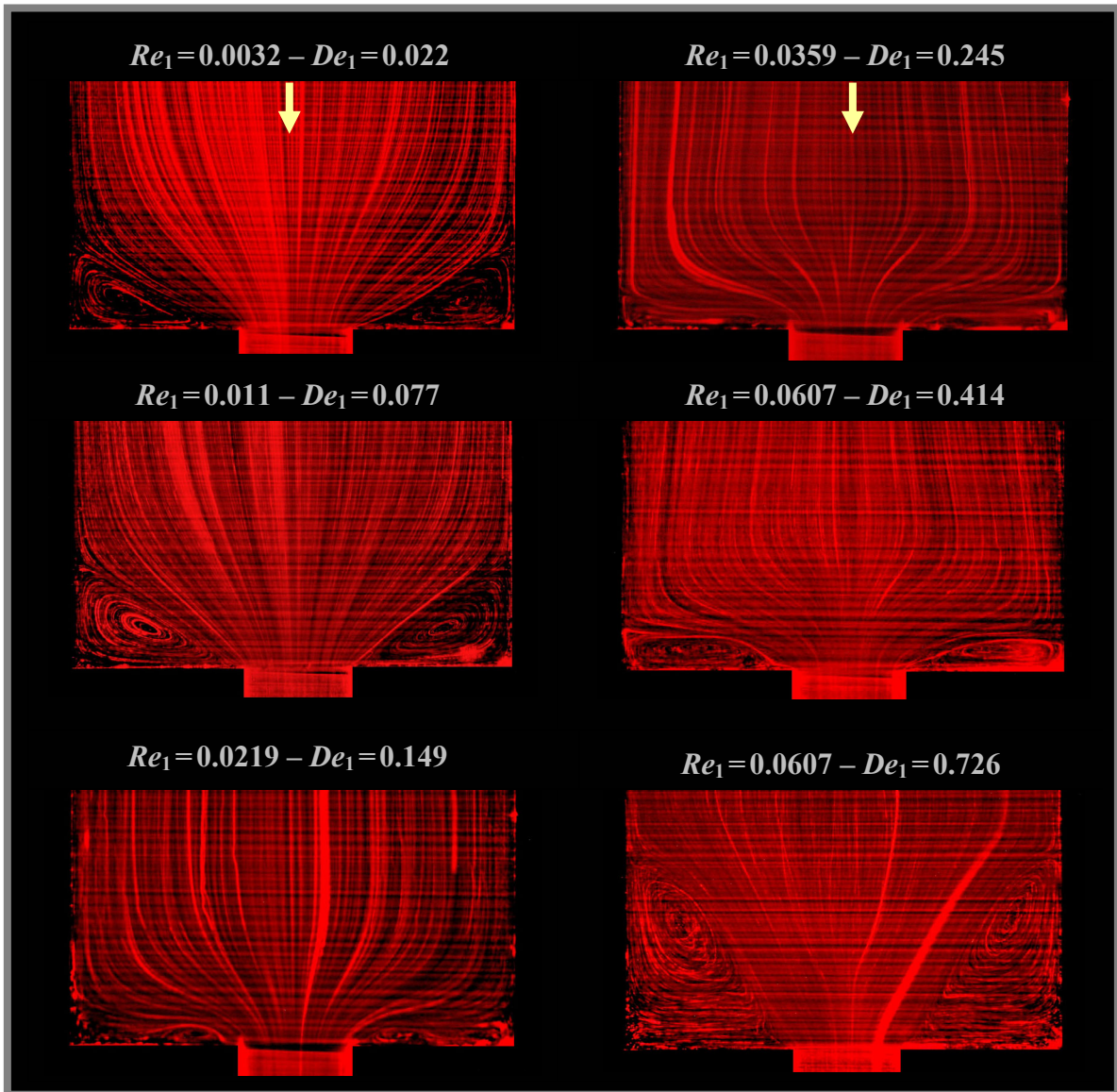


Figure 7- Influence of elasticity on the streakline flow patterns at the middle plane of a 4:1:1 contraction for PAA300.

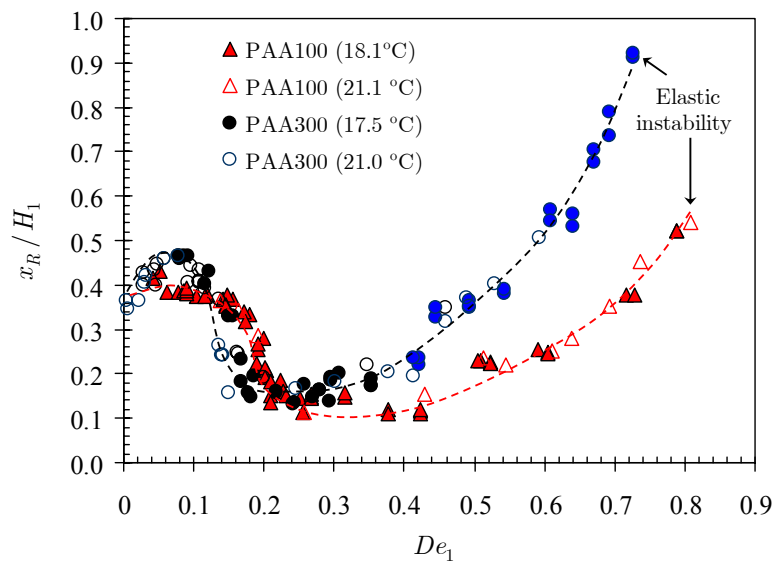


Figure 8- Variation of normalized vortex length with flow elasticity for Boger fluids PAA100 and PAA300.

6. References

- Alves, M. A. 2004, “Escoamentos de fluidos viscoelásticos em regime laminar: análise numérica, teórica e experimental.”, PhD thesis, University of Porto, Portugal.
- Alves, M. A., Oliveira, P. J. and Pinho, F. T., 2003a, "Benchmark solutions for the flow of Oldroyd-B and PTT fluids in planar contractions", *J. Non-Newt. Fluid Mech.*, vol. 110, pp. 45-75.
- Alves, M. A., Oliveira, P. J. and Pinho, F. T., 2003b, “Numerical simulation of viscoelastic contraction flows”, *Proceedings of Second M. I. T. Conference on Computational Fluid and Solid Mechanics*, Edited by KJ Bathe, Boston, 17-20 June 2003, USA, pp 826-829.
- Alves, M. A., Pinho, F. T. and Oliveira, P. J. 2000, “Effect of a high-resolution differencing scheme on finite-volume predictions of viscoelastic flows”, *J. Non-Newt. Fluid Mech.*, vol. 93, pp. 287-314.
- Barnes, H. A. 2000, “A handbook of elementary rheology”, *Institute of Non-Newtonian Fluid Mechanics*, Aberystwyth, University of Wales.
- Boger, D.V., 1987, “Viscoelastic flows through contractions”, *Annual Rev. Fluid Mech.*, vol. 19, pp. 157-182.
- Boger, D.V., Hur, D.U. and Binnington, R.J., 1986, “Further observations of elastic effects in tubular entry flows”, *J. Non-Newt. Fluid Mech.*, vol. 20, pp. 31-49.
- Cable, P.J. and Boger, D.V., 1978a, “A comprehensive experimental investigation of tubular entry flow of viscoelastic fluids: Part I. Vortex characteristics in stable flow. *AIChEJ*, vol. 24, pp. 868-879.
- Cable, P.J. and Boger, D.V., 1978b, “A comprehensive experimental investigation of tubular entry flow of viscoelastic fluids: Part II. The velocity fields in stable flow. *AIChEJ*, vol. 24, pp. 992-999.
- Cable, P.J. and Boger, D.V., 1979, “A comprehensive experimental investigation of tubular entry flow of viscoelastic fluids: Part III. Unstable flow. *AIChEJ*, vol. 25, pp. 152-159.
- Evans, R.E. and Walters, K., 1986, “Flow characteristics associated with abrupt changes in geometry in the case of highly elastic liquids” *J. Non-Newt. Fluid Mech.*, vol. 20, pp 11-29.
- Evans, R.E. and Walters, K., 1988, “Further remarks on the lip-vortex mechanism of vortex enhancement in planar contraction flows” *J. Non-Newt. Fluid Mech.*, vol. 32, pp. 95-105.
- Hassager, O., 1988, “Working group on numerical techniques. Fifth International Workshop on Numerical Methods in Non-Newtonian Flows, Lake Arrowhead, USA” *J. Non-Newt. Fluid Mechanics*, vol. 29, pp. 2-5.
- McKinley, G. H., Raiford, W. P., Brown, R. A. and Armstrong, R. C. 1991, “Non linear dynamics of viscoelastic flow in axisymmetric abrupt contractions”, *J. Fluid Mechanics*, vol. 223, pp 411-456.
- Nguyen, H. and Boger, D.V., 1979, “The kinematics and stability of die entry flows” *J. Non-Newt. Fluid Mech.*, vol. 5, pp.353-368.
- Nigen, S. and Walters, K., 2002, "Viscoelastic contraction flows: comparison of axisymmetric and planar configurations" *J. Non-Newt. Fluid Mech.*, vol. 102, pp. 343-359.
- Purnode, B. and Crochet, M. J. 1996, "Flows of polymer solutions through contractions. Part 1: flows of polyacrylamide solutions through planar contractions" *J. Non-Newt. Fluid Mech.*, vol. 65, pp. 269-289.
- Quinzani, L. M., Armstrong, R.C. and Brown, R. A. 1994, “Birefringence and laser-Doppler velocimetry (LDV) studies of viscoelastic flow through a planar contraction” *J. Non-Newt. Fluid Mech.*, vol. 52, pp. 1-36.
- Stokes, J. R. 1998, “Swirling flow of viscoelastic fluids”, PhD thesis, Department of Chemical Engineering, University of Melbourne, Australia.
- Walters, K. and Rawlinson, D.M., 1982, “On some contraction flows for Boger fluids”, *Rheol. Acta*, vol. 21, pp. 547-552.
- Walters, K. and Webster, M.F., 1982, “On dominating elastico-viscous response in some complex flows”, *Phil. Trans. R. Soc. London A*, vol. 308, pp. 199-218.
- Walters, K. and Webster, M. F., 2003, “The distinctive CFD challenges of computational rheology”, *Int. J. Num. Meth. Fluids*, vol. 43, pp. 577-596.
- White, S. A. and Baird, D. G. 1988, “Flow visualization and birefringence studies on planar entry flow behavior of polymer melts”, *J. Non-Newtonian Fluid Mechanics*, vol. 29, pp. 245-267.

7. Copyright Notice

The authors are the only responsible for the printed material included in this paper.